tortion of the lattice by the magnetic ion if this distortion leaves the symmetry unchanged.

We also note that these relations are also correct in the "overlap" approximation for the covalency, because as long as only Coulombian energy is considered, the Laplace equation becomes then $\nabla^2 V = 4\pi\rho$, ρ being the spherical charge density, and only the radial part of the expansion (1) is modified.[11] Obviously, if exchange forces are included, our description is not valid.

[11] This point was called to our attention by Dr. D. K. Ray.

In addition to the reduction of the number of parameters, this work establishes formulas [(13) and (15)] which, once the standard combinations $Y(l,\Gamma_\alpha,a,\beta)$ and $T(\Gamma_\alpha,b,\beta)$ are known, gives, for any environment, the values of the parameters with a minimum amount of calculation.

ACKNOWLEDGMENT

It is a pleasure for the authors to thank Dr. D. K. Ray for reading the manuscript.

PHYSICAL REVIEW B VOLUME 1, NUMBER 9 1 MAY 1970

Angle Dependence of Paramagnetic-Resonance Line Intensities of Trivalent Cr^{53} in MgO†

D. H. DICKEY* AND JOHN E. DRUMHELLER
Department of Physics, Montana State University, Bozeman, Montana 59715
(Received 14 November 1969)

Three methods have been used to predict paramagnetic-resonance line intensities in the spectrum of trivalent Cr^{53} in sites of tetragonal symmetry in MgO. The methods are: numerical diagonalization of the Hamiltonian matrix, perturbation theory, and a technique involving the magnetic field induced at the nucleus by the electron spin. Experimentally observed line intensities are compared with the calculated intensities. The induced-field method is found to adequately describe the spectrum and to agree very closely with results from numerical diagonalization of the Hamiltonian. Some small discrepancies in line positions are observed which imply an inaccuracy in the usual axial-field spin Hamiltonian.

I. INTRODUCTION

THE angular dependence of transition probabilities in electron paramagnetic resonance (EPR) becomes complicated when the applied magnetic field and crystalline electric field compete as a quantization axis in the presence of a hyperfine interaction. Additional transitions are observable because the states may be mixed by matrix elements of the hyperfine interaction and crystal field operators. The magnetic dipole selection rule ($\Delta M = \pm 1$) is valid if applied to the base states $|M_S,M_I\rangle = |M,m\rangle$, but breaks down completely at some orientations if applied to the mixed states. This results in the appearance of so-called forbidden hyperfine lines in the EPR spectrum. For the case of small crystalline field splittings, adequate explanations of the existence of these forbidden transitions using perturbation techniques have been given by previous authors,[1,2] particularly for the ions of manganese and vanadium.

For the cases where the crystalline field splitting is comparable to or larger than the Zeeman splitting, the angle-dependent spectrum is very complicated and only direct diagonalization of the full Hamiltonian is adequate. For the intermediate cases Bir[3] and Bir and Sochava[4] have developed a technique which we call the induced-field method, which relies on the calculation of the magnetic field induced at the nucleus by the electron spin. In the induced-field method, either perturbation theory or diagonalization techniques may be employed but in either case only on the electronic portion of the Hamiltonian. The present work was done at X-band frequencies, for which the Zeeman splitting is about twice that of the crystal field. It successfully uses the induced-field method to explain the angular dependence of the Cr^{53} spectra in the tetragonal sites of magnesium oxide. It is the first report of chromium-forbidden hyperfine transitions.

The EPR spectrum of trivalent chromium is readily observed in ionic crystals and has been extensively studied, particularly as a dilute impurity in aluminum oxide[5,6] and magnesium oxide.[7,8] The latter crystal is

† Work supported by the National Science Foundation.
* Present address: Bell & Howell Research Laboratories, Pasadena, Cal. 91109.
[1] B. Bleaney and R. Rubins, Proc. Phys. Soc. (London) **77**, 103 (1961).
[2] J. E. Drumheller and R. Rubins, Phys. Rev. **133**, A1099 (1964).
[3] G. L. Bir, Fiz. Tverd. Tela **5**, 2236 (1963) [Soviet Phys. Solid State **5**, 1628 (1964)].
[4] G. L. Bir and L. S. Sochava, Fiz. Tverd. Tela **5**, 3594 (1963) [Soviet Phys. Solid State **5**, 2637 (1964)].
[5] A. A. Manenkov and A. M. Prohorov, Zh. Eksperim. i Teor. Fiz. **31**, 346 (1956] [Soviet Phys. JETP **4**, 288 (1957)].
[6] R. W. Terhune, J. Lambe, C. Kikuchi, and J. Baker, Phys. Rev. **123**, 1265 (1961).
[7] J. E. Wertz and P. Auzins, Phys. Rev. **106**, 484 (1957).
[8] S. A. Marshall, J. A. Hodges, and R. A. Serway, Phys. Rev. **136**, A1024 (1964).

cubic, so unless the chromium ion is associated with a lattice defect, its ground state is degenerate and the resonance spectrum is an uninteresting single line. Trivalent chromium in MgO often occurs, though, in association with a next-nearest-neighbor cation vacancy.[7] The resulting tetragonal distortion produces a ground-state splitting and a more complicated spectrum.[9] For the isotope Cr^{53} ($I=\frac{3}{2}$), the spectrum is further complicated by the hyperfine interaction.[10]

The ground state of trivalent Cr^{53} in MgO consists of 16 levels, so that a total of 120 transitions can occur within the ground state, ignoring selection rules. Twenty-four of these are NMR transitions. We have observed most of the transitions but have concentrated on those 16 characterized by $M,m=+\frac{1}{2}, m\rightarrow-\frac{1}{2}$, m' (m and $m'=\frac{3}{2}, \frac{1}{2}, -\frac{1}{2}, -\frac{3}{2}$). There is some lack of agreement between observed and calculated line positions and intensities, and this is attributed to the omission of some unknown term in the spin Hamiltonian.

II. CALCULATION OF LINE INTENSITIES

Relative line intensities in an EPR spectrum may be found from the matrix elements of the microwave field operator:

$$I \propto |\langle\Psi_f|g\beta\mathbf{H}_{rf}\cdot\mathbf{S}|\Psi_i\rangle|^2. \quad (1)$$

The wave functions used to calculate these matrix elements are the eigenfunctions of the spin Hamiltonian of the paramagnetic ion. For a chromium ion in a crystal field of tetragonal symmetry, the appropriate spin Hamiltonian is

$$\mathcal{H}=\beta\mathbf{H}\cdot\mathbf{g}\cdot\mathbf{S}+D[S_{z'}{}^2-\tfrac{1}{3}S^2]+\mathbf{S}\cdot\mathbf{A}\cdot\mathbf{I}-\beta_N\mathbf{H}\cdot\mathbf{g}_N\cdot\mathbf{I}, \quad (2)$$

where the primed coordinate refers to the crystal field direction. The nuclear quadrupole interaction is omitted since there is no experimental evidence that it is strong enough to be observable. In a very intense magnetic field the 16 basis vectors $|S,M,I,m\rangle=|M,m\rangle$ are eigenfunctions of the Hamiltonian. For usual laboratory fields, the second and third terms of Eq. (2) are not negligible and the correct wave functions may be complicated mixtures of the basis vectors.

The three methods used to calculate the wave functions and subsequent line intensities are each discussed below.

A. Direct Diagonalization

A numerical diagonalization of the Hamiltonian matrix, using a digital computer, is the most straightforward and accurate method of obtaining the necessary wave functions. In addition, the eigenvalues obtained with this method can be used to determine exact line positions. Comparing the computed line positions with those observed then becomes a test of the accuracy and validity of the spin Hamiltonian.

TABLE I. Summary of Hamiltonian parameters.

Parameter	Temperature (°K)		Reference
$g_{\parallel}$	300	1.97882±0.0001	This work
	77	1.97854±0.00005	8
	300	1.9782	7
$g_{\perp}$	300	1.98200±0.001	This work
	77	1.98171±0.00005	8
D	300	−887.1±0.1 G	This work
	77	−879.76±0.04	8
	300	−887.0	7
A	300	17.84±0.1 G	This work
	77	17.73±0.02	8
	300	17.85	7
μ_N ($=\frac{3}{2}g_N$)	4.2	0.4751±0.0005	12

Values for $g_{\parallel}$, $g_{\perp}$, D, and A were determined from measurements of line positions with the magnetic field parallel and perpendicular to the crystal axis. In these orientations the Cr^{52} Hamiltonian matrix factors, so that all the parameters in the Hamiltonian can be determined before starting the computer diagonalization.[11] The parameters we obtain are shown in Table I along with the results of other workers.[12] Experimental accuracy was not sufficient to permit the detection of any slight anisotropy[8] in the hyperfine interaction.

Resonance line positions are not usually found using a numerical diagonalization because the resonance field itself must be known before the matrix can be diagonalized. We use an iterative process though, which begins by diagonalizing the Hamiltonian with an assumed value for H. The microwave photon energy is then compared to the difference in energy between the appropriate pair of eigenvalues. The excess photon energy (measured in G) is added to the assumed value of H and the matrix is rediagonalized. The iteration is continued until energy is conserved. Convergence is rapid, so only a few iterations are required to define a line position with the necessary accuracy, but the process must be repeated for each orientation and each transition.

The line intensity in each case is calculated from Eq. (1) using the eigenvectors stored in the computer after the final diagonalization. Relative line intensities were obtained in this way for the 16 lines in the $M=+\frac{1}{2}\rightarrow-\frac{1}{2}$ group for $\theta=30°$ and $\theta=45°$. Some of these results are plotted in Figs. 1 and 2 for comparison with the results of the other methods.

B. Induced-Field Method of Bir

With the assumption that the wave functions in Eq. (1) are separable into electronic and nuclear parts, the

[9] P. Auzins and J. E. Wertz, J. Chem. Phys. **43**, 1229 (1965).
[10] W. Low, Phys. Rev. **105**, 801 (1957).
[11] The small isotope effect (see Ref. 8) was ignored, and the Hamiltonian for Cr^{53} was assumed to be identical with that for Cr^{52} except for addition of the hyperfine interaction. Spectra of both isotopes were observable in the crystal.
[12] G. A. Woonton and G. L. Dyer, Can. J. Phys. **45**, 2265 (1967).

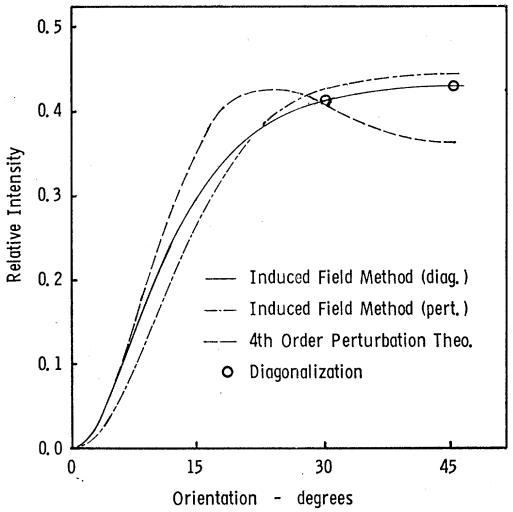

FIG. 1. Calculated intensity of the $m=-\frac{3}{2}\rightarrow-\frac{1}{2}$ forbidden line as a function of the angle between external field and crystal axis.

relative line intensity can be written

$$I_{Mm,M'm'}=|g\beta H_{\mathrm{rf}}\langle\psi_{M'}|S_y|\psi_M\rangle|^2|\langle\phi_{m'}{}^{M'}|\phi_m{}^M\rangle|^2, \quad (3)$$

where

$$\Psi_{M,m}=\psi_M\phi_m{}^M,$$

ψ_M being the electronic wave function and $\phi_m{}^M$, the nuclear wave function. This separation can be made if one retains the M index on the nuclear functions. That is, the electronic-spin functions are virtually independent of the nuclear state because the hyperfine energy is so much less than the electronic Zeeman energy or crystal field potential. In the absence of a quadrupole interaction the nuclear-spin functions $\phi_m{}^M$ are eigenfunctions of the operator I_ζ, where ζ is the direction of the effective magnetic field at the nucleus.

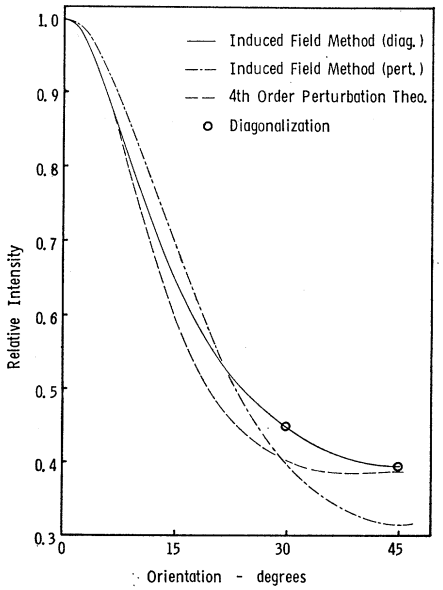

FIG. 2. Calculated intensity of the $m=-\frac{3}{2}\rightarrow-\frac{3}{2}$ allowed line as a function of the angle between external field and crystal axis.

TABLE II. Rotation operators for the four-dimensional vector space.

$R_{\frac{3}{2},\frac{3}{2}}{}^2=\frac{1}{8}(1+\mu)^3$	$R_{\frac{3}{2},\frac{1}{2}}{}^2=\frac{3}{8}(1+\mu)^2(1-\mu)$
$R_{\frac{3}{2},-\frac{1}{2}}{}^2=\frac{3}{8}(1-\mu)^2(1+\mu)$	$R_{\frac{3}{2},-\frac{3}{2}}{}^2=\frac{1}{8}(1-\mu)^3$
$R_{\frac{1}{2},\frac{1}{2}}{}^2=\frac{1}{8}(1+\mu)(1-3\mu)^2$	$R_{\frac{1}{2},-\frac{1}{2}}{}^2=\frac{1}{8}(1-\mu)(1+3\mu)^2$

For a given value of M, the $\phi_m{}^M$'s are orthogonal and can be related to those of a different value of M with a rotation operator

$$\phi_m{}^M=\sum_{m'}R_{mm'}(\alpha_{MM'})\phi_{m'}{}^{M'}, \quad (4)$$

where $\alpha_{MM'}$ is the angle between the quantization axes for the two sets of nuclear-spin functions and $R(\alpha)$ is the rotation operator which relates these sets. The squared scalar product of Eq. (3) now reduces to

$$|\langle\phi_{m'}{}^{M'}|\phi_m{}^M\rangle|^2=R_{mm'}{}^2(\alpha_{MM'}). \quad (5)$$

The general form of the R functions is known,[13] and for the four-dimensional vector space appropriate to a nuclear spin of $\frac{3}{2}$, they have the specific form shown in Table II, where $\mu=\cos\alpha_{MM'}$.

The nuclear-spin quantization axes referred to above are the directions of the magnetic fields seen by the nucleus. These fields are the vector sum of the external field and the field induced at the nucleus by the electron spin. The angles relating these fields are shown in Fig. 3. The induced field is not in general parallel to the external field owing to the influence of the crystal potential upon the electronic states. The components of the induced field and hence its direction can be found by considering the equivalence between the hyperfine

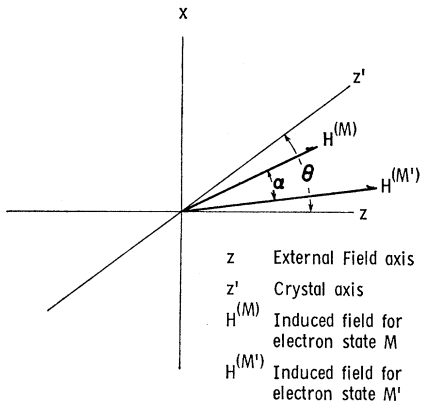

FIG. 3. Plan view of the xz plane, showing induced fields and angles referred to in the text.

[13] I. Gel'fand, R. Minlos, and Z. Shapiro, *Representations of the Rotation and Lorentz Groups* (Macmillan, New York, 1963), Sec. 7, or see Ref. 3.

energy and the Zeeman energy of the nucleus in the induced field,

$$g_N\beta_N\mathbf{H}(\text{ind})\cdot\mathbf{I}=A\mathbf{S}\cdot\mathbf{I}, \quad (6)$$

so that the components of $\mathbf{H}$(ind) are

$$H_i^M(\text{ind})=(A/g_N\beta_N)\langle\psi_M|S_i|\psi_M\rangle, \quad i=x, y, z. \quad (7)$$

The magnitude of the induced field is on the order of the coefficient $A/g_N\beta_N$ (about 200 kG), so that the external field may be neglected in further calculations. With the given coordinate system, the induced field will always lie in the xz plane, so that the angle $\alpha_{MM'}$ is readily found to be:

$$\alpha_{MM'}=\tan^{-1}H_x^M/H_z^M-\tan^{-1}H_x^{M'}/H_z^{M'}. \quad (8)$$

The following approach may now be used for finding the intensity of a given line: Electron-spin wave functions are found and used to calculate expectation values for S_x and S_z for initial and final states. Equation (7) is then applied and the angle $\alpha_{MM'}$ is determined. The scalar product of nuclear-spin functions is then found according to Eq. (5) and finally substituted in Eq. (3) for the intensity. Bir has pointed out that the strong angular dependence of line intensity is almost completely attributable to the angular dependence of the scalar product of nuclear-spin functions. The electronic transition matrix element of Eq. (3) usually has only a weak angular dependence.

Two methods were used for finding electronic wave functions. First-order perturbation theory was used to generate approximate functions, and these predicted line intensities that compared within experimental error to observed intensities. For an accurate comparison of this method to that using direct diagonalization of the full matrix, wave functions were also obtained from a numerical diagonalization of the 4×4 electronic Hamiltonian matrix. This approach resulted in line intensities that agreed within less than 1% with those obtained from the full matrix, at the test angles of 30° and 45°. The line intensities obtained with both methods are plotted in Figs. 1 and 2.

C. Perturbation Theory

Following the approach used by Lyons and Kedzie[14] for the calculation of energy levels, we have included all of the diagonal parts of the crystal field potential and the hyperfine interaction in the unperturbed Hamiltonian. This approach has the advantage that since the perturbation has only off-diagonal matrix elements, the number of third- and fourth-order terms is greatly reduced. The energy denominators in the terms that remain are more complicated, but can be expanded to give the usual series in $1/g\beta H$. The Appendix contains an outline of the wave-function calculations, as well as explicit expressions for the admixture of neighboring hyperfine states for the case $A\ll D,H$.

A disadvantage of the perturbation technique is that the wave functions one obtains are not normalized. They can be normalized, but only if all 15 admixtures are calculated. This problem can be circumvented by calculating line intensities with the unnormalized wave functions and then normalizing the intensities. Ideally, the intensity of all 96 EPR lines should be included in the normalization, but in practice it is found that only four lines need to be considered at one time. For example, the four lines $+\frac{1}{2},+\frac{3}{2}\rightarrow-\frac{1}{2},m$ ($m=\frac{3}{2}, \frac{1}{2}, -\frac{1}{2}, -\frac{3}{2}$) are assumed to have constant total intensity, and their relative strengths as a function of angle may be readily found. This is the same kind of normalization which is implicit in the induced-field method, except here the variation of Cr^{52} line intensity is ignored. Intensities obtained from the perturbation method are plotted in Figs. 1 and 2 for the $+\frac{1}{2}, -\frac{3}{2}\rightarrow-\frac{1}{2}, -\frac{1}{2}$ and $+\frac{1}{2}, -\frac{3}{2}\rightarrow-\frac{1}{2}, -\frac{3}{2}$ lines.

III. OBSERVED SPECTRA

The experimental results were obtained using a superheterodyne spectrometer employing balanced mixer detection and field modulation. The spectrometer was operated at a frequency of 9.994 GHz, and the data were recorded at room temperature.

The crystal we used was doped with enriched Cr^{53}, so that approximately two-thirds of the chromium ions are Cr^{53} and one-third Cr^{52}. (Cr^{53} natural abundance is 9%.) There are four times as many Cr^{53} lines, so that each one is still only about one-half the intensity of the equivalent Cr^{52} line. The resulting spectrum consists of groups of four Cr^{53} hyperfine components with the equivalent Cr^{52} line standing in the center of each group. As the magnetic field is rotated away from a crystal axis, the four Cr^{53} lines rapidly lose intensity while forbidden lines appear in the spectrum. Observation of the spectrum is not possible at many orientations, owing to the presence of intense lines belonging to the spectra of other paramagnetic impurities in the crystal.

For the magnetic field at an angle of 45° from the tetragonal axis the $M=+\frac{1}{2}\rightarrow-\frac{1}{2}$ group of lines is not obstructed by other lines and appears as shown in Fig. 4(a). At this orientation the ground-state wave functions are mixed so completely that the forbidden lines have intensity greater than the allowed lines. Line positions and intensities calculated by diagonalization of the full matrix are shown for comparison in Fig. 4(b). The calculated forbidden doublet splittings at 45° are all significantly less than the line widths, so the line intensities have been merely added to construct Fig. 4(b). Note that the $m=\pm\frac{1}{2}\rightarrow\pm\frac{1}{2}$ allowed lines nearly vanish at this orientation.

Measurements of line intensities within the $M=+\frac{1}{2}\rightarrow-\frac{1}{2}$ group for the $m=-\frac{3}{2}\rightarrow-\frac{3}{2}$ allowed line and the neighboring $m=-\frac{3}{2}\rightarrow-\frac{1}{2}$ forbidden

[14] D. H. Lyons and R. W. Kedzie, Phys. Rev. 145, 148 (1966).

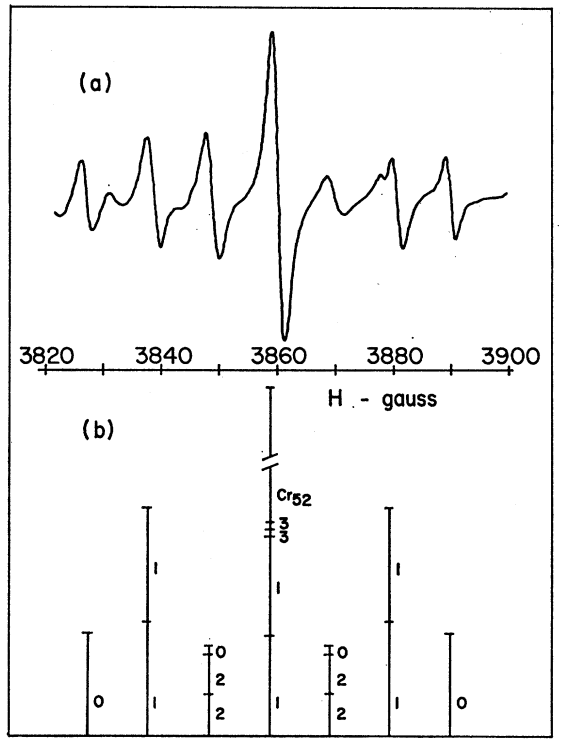

FIG. 4. The $M=+\frac{1}{2}\rightarrow-\frac{1}{2}$ spectrum for $\theta=45°$. (a) Observed first derivative spectrum: The line near 3850 G is a superposition of an extraneous Cr^{52} line and three Cr^{53} lines, and is therefore more intense than its counterpart near 3870 G. (b) Calculated: The number to the right of each line is the change in nuclear-spin magnetic quantum number, e.g., the leftmost line is the $\Delta m=0$ ($m=\frac{3}{2}\rightarrow\frac{3}{2}$) transition.

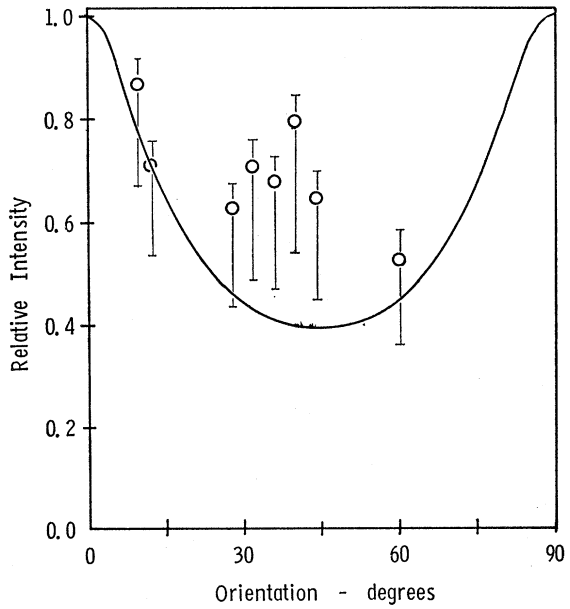

FIG. 5. Intensity as a function of orientation for the $m=-\frac{3}{2}\rightarrow-\frac{3}{2}$ allowed line. Solid line: calculated with induced field method. Points: observed intensity.

doublet have been made at all orientations at which they could be observed. These results are plotted in Figs. 5 and 6. The measurements were made relative to the intensity of the corresponding Cr^{52} line. The Cr^{52} line intensity was corrected for the presence of the forbidden doublet which occurs at about the same field. Errors in the experimental measurements occur because the lines are weak and because of the proximity of strong extraneous lines nearby.

The Hamiltonian we use does not predict a significant angular dependence in the forbidden doublet splittings. We observe, however, that the $m=+\frac{3}{2}\rightarrow+\frac{1}{2}$ doublet splitting does vary rapidly (from 4 G to zero) between 30° and 45°. The $m=-\frac{3}{2}\rightarrow-\frac{1}{2}$ doublet appears to have nearly zero splitting at all orientations, and this

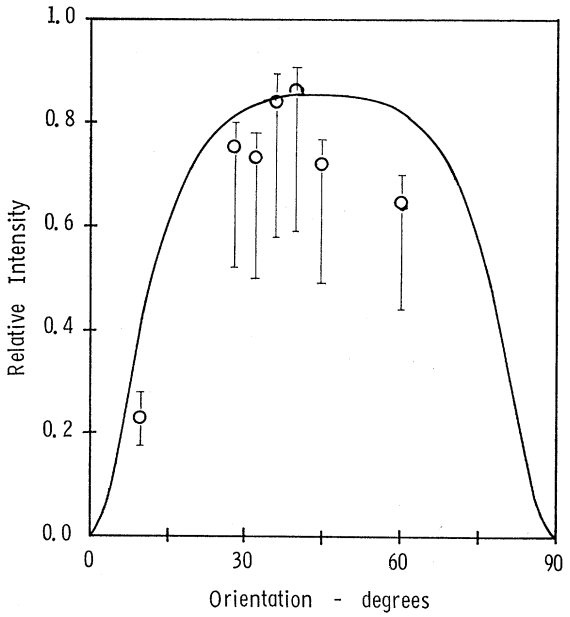

FIG. 6. Intensity as a function of orientation for the unresolved $m=-\frac{3}{2}\leftrightarrow-\frac{1}{2}$ forbidden doublet. Solid line: calculated with induced-field method. Points: observed intensity.

difference in itself is anomalous. The inclusion of a quadrupole term in the Hamiltonian would introduce an angular dependence, but should affect both the above doublets equally. Evidently there is an additional interaction in effect here which is not usually encountered.

IV. CONCLUSION

We have shown that for systems which have reasonably large crystal field splittings, a good qualitative description of the angular dependence of EPR line intensities can be easily achieved by using the induced-field method of Bir and electronic wave functions calculated from low-order perturbation theory. The induced-field method becomes very exact if more accurate electronic wave functions are used. We have

carried the perturbation approach of Bleaney and Rubins to fourth order and, although the series do converge with such large crystal field splittings, the results are not exact enough to justify the labor involved.

The spin Hamiltonian predicts Cr^{52} line positions remarkably well at all angles, but is in error by several G on some of the forbidden lines in the Cr^{53} spectrum. Further investigation of the discrepancies is planned, with the hope that their empirical description will suggest a theoretical explanation.

The methods used in this work may be applied to similar systems such as V^{51} or Fe^{57}, noting that a different set of rotation operators is necessary if the nuclear spin is other than $\frac{3}{2}$.

APPENDIX

If the perturbation Hamiltonian is nondiagonal, the series expression for the wave function is

$$\Psi_n=|n\rangle+\sum_p|p\rangle\left\{\frac{H_{pn}}{E_{np}}+\sum_q\left[\frac{H_{pq}H_{qn}}{E_{np}E_{nq}}-\frac{H_{pn}H_{qn}{}^2}{E_{np}{}^2E_{nq}}\right.\right.$$
$$+\sum_r\left(\frac{H_{pq}H_{qr}H_{rn}}{E_{np}E_{nq}E_{nr}}-\frac{H_{pq}H_{qn}H_{rn}{}^2}{E_{np}E_{nq}{}^2E_{nr}}\right.$$
$$\left.-\frac{H_{pq}H_{qn}H_{rn}{}^2}{E_{np}{}^2E_{nq}E_{nr}}-\frac{H_{pn}H_{nq}H_{qr}H_{rn}}{E_{np}{}^2E_{nq}E_{nr}}\right.$$
$$\left.\left.\left.+\sum_s\frac{H_{pq}H_{qr}H_{rs}H_{sn}}{E_{np}E_{nq}E_{nr}E_{ns}}+\cdots\right)\right]\right\}, \quad \text{(A1)}$$

where all sums exclude n, and the energy denominators are differences in zero-order energies. For instance, with the Hamiltonian of Eq. (2), the zero-order energy for the state labeled M,m is

$$E_{M,m}=g\beta HM+AMm+DP_2(\cos\theta)$$
$$\times[M^2-\tfrac{1}{3}S(S+1)]-g_N\beta_NHm, \quad \text{(A2)}$$

and the perturbation Hamiltonian is

$$\mathcal{H}=\tfrac{1}{2}A(S_+I_-+S_-I_+)+\tfrac{1}{4}D[\sin^2\theta\,(S_+{}^2+S_-{}^2)$$
$$+\sin2\theta\,(S_zS_++S_zS_-+S_+S_z+S_-S_z)]. \quad \text{(A3)}$$

We wish to calculate the admixture of neighboring and next-neighboring hyperfine states. That is, if n is M,m, then we wish to evaluate Eq. (A1) for $p=M,m\pm1$ and $M,m\pm2$. Only five of the eight terms in the large curly bracket will contribute for neighboring state admixture, and only two will contribute for second-neighboring states. If $r=p$ in the last term, a large contribution (of order AD^3/A^2H^2) results, but is cancelled to within terms of order D^3/H^3 by the third from last term. Writing the abbreviated wave function

$$\Psi_{M,m}=|M,m\rangle+\alpha|M,m-1\rangle+\beta|M,m+1\rangle$$
$$+\gamma|M,m-2\rangle+\delta|M,m+2\rangle, \quad \text{(A4)}$$

we find the following expressions for the admixture coefficients, evaluated for $S=\frac{3}{2}$ and $M=\pm\frac{1}{2}$:

$$\alpha=\frac{3D\sin2\theta}{4g\beta H}[I(I+1)-m(m-1)]^{1/2}$$
$$\times\left[\mp2+\frac{D}{g\beta H}(4-9\sin^2\theta)\right.$$
$$\left.\pm\frac{D^2}{8(g\beta H)^2}(-64+79\sin^22\theta-13\sin^4\theta)\right],$$
$$\beta=-\alpha[I(I+1)-m(m+1)]^{1/2}/$$
$$[I(I+1)-m(m-1)]^{1/2},$$
$$\gamma=\frac{3D\sin2\theta}{4g\beta H}[I(I+1)-m(m-1)]^{1/2} \quad \text{(A5)}$$
$$\times[I(I+1)-(m-1)(m-2)]^{1/2}$$
$$\times\left[\frac{3D\sin2\theta}{2g\beta H}\mp\frac{A\tan\theta}{4g\beta H}\right],$$
$$\delta=\frac{3D\sin2\theta}{4g\beta H}[I(I+1)-m(m+1)]^{1/2}$$
$$\times[I(I+1)-(m+1)(m+2)]^{1/2}$$
$$\times\left[\frac{3D\sin2\theta}{2g\beta H}\pm\frac{A\tan\theta}{4g\beta H}\right],$$

where the upper signs are for $M=+\frac{1}{2}$, and the lower signs for $M=-\frac{1}{2}$.

There is significant admixture of other than neighboring hyperfine states, but they do not contribute greatly to the intensity of the forbidden hyperfine transitions.